JOURNAL OF EXPERIMENTAL AND THEORETICAL PHYSICS, 2024, Vol. 166, No. 1(7), pp. 83–91

SUPERCONDUCTIVITY AND INHOMOGENEOUS STATES IN METALLIC HYDROGEN AND ELECTRONIC SYSTEMS WITH ATTRACTION

© 2024 M. Yu. Kagan[a,b*], R. Sh. Ikhsanov[a,c], I. A. Kovalev[a], A. V. Krasavin[d], E. A. Mazur[d,e]

[a]National Research University Higher School of Economics 101000, Moscow, Russia
[b]Kapitza Institute for Physical Problems of the Russian Academy of Sciences 119334, Moscow, Russia
[c]Lebedev Physical Institute of the Russian Academy of Sciences 119991, Moscow, Russia
[d]National Research Nuclear University MEPhI 115409, Moscow, Russia
[e]National Research Center Kurchatov Institute 123182, Moscow, Russia

*e-mail: kagan@kapitza.ras.ru

Received February 21, 2024
Revised March 12, 2024
Accepted March 13, 2024

Abstract. Superconductivity and inhomogeneous states in metallic hydrogen and several electronic systems with attraction, described by inhomogeneous (spatially separated) Fermi–Bose mixture with superconducting clusters or order parameter droplets in a matrix of unpaired normal states, have been considered. The spatially separated Fermi–Bose mixture is realized in bismuth oxide superconductors $BaKBiO_3$. Order parameter droplets can appear in thin films of "dirty" (with high impurity content) metal, described by a two-dimensional Hubbard model of low electron density with strong attraction and strong diagonal disorder. In metallic hydrogen and metal hydrides, droplets and large percolation clusters can form in shock wave experiments near the first-order phase transition boundary between liquid (non-crystalline) metallic and dielectric phases. For homogeneous superconductivity in metallic hydrogen and metal hydrides, within the framework of generalized Eliashberg equations, new results were obtained demonstrating negative sign of derivative $dT_c / dP < 0$, for the pressure range from 60 to 100 hPa in triple hydride $LaBH_8$. From the perspective of unusual physical properties, both in normal and possibly superfluid ("supersolid") states, important analogies between metallic hydrogen and quantum crystals have been highlighted.

Article for the special issue of JETP dedicated to the 130th anniversary of P. L. Kapitsa

DOI: 10.31857/S004445102407e095

1. INTRODUCTION

The paper [1] first formulated the idea of spatially separated Fermi–Bose mixture of local bosonic clusters or complexes (containing compact electronic or hole pairs) in a matrix of unpaired (Fermi-liquid) states to explain the mechanism of superconductivity and the nature of electronic transport in the normal state in bismuth oxides $BaKBiO_3$.

Fig. 1 shows a scheme of the local crystal structure in the plane of BiO_2 in the initial compound $BaBiO_3$, which is a CDW-insulator with a checkerboard structure of octahedra distribution BiL_2O_6 and BiO_6 (left figure), and the local crystal structure $Ba_{0.5}K_{0.5}BiO_3$ with diagonal chains of complexes BiO_6, embedded in a large percolation cluster of octahedra BiL_2O_6 (right figure) [2].

Note that the emergence of long-range order and macroscopic wave function of the superconducting state in $Ba_{1-x}K_xBiO_3$ is due to tunneling of local electron pairs from one bosonic cluster BiO_6 to the adjacent BiO_6 cluster through a tunnel barrier formed by normal fermionic clusters. The components of the Fermi–Bose mixture in the range of metallic

concentrations $0.37 < x < 0.5$ are separated in real space but not separated in energy space (see more detailed description in [1, 2]).

Also note that the formation of metallic ferromagnetic nanoscale droplets in nonmagnetic (paramagnetic, antiferromagnetic, and charge-ordered) dielectric matrices in magnetic oxides was discussed in detail in [3].

In this mini-review, we develop ideas first formulated in papers [1–3] for bismuth oxides and manganites, and generalize them to superconducting droplets (order parameter droplets) emerging in thin films of a "dirty" metal, described by a two-dimensional Hubbard model of low electron density with strong attraction in the presence of strong random potential.

In this system, the percolation nature of the insulator-superconductor phase transition is also interesting when forming a large cluster of branched droplet structures (having the shape of "trees") when approaching the critical electron concentration.

In the second part of the mini-review, we analyze various possibilities for enhancing superconductivity and reducing pressure (searching for long-lived metastable phases) in metallic hydrogen and metal hydrides, related, in particular, to the more complex nature (chemical composition) of these compounds.

The main new result here is the demonstration of the negative sign of the critical temperature derivative with respect to pressure, $dT_c / dP < 0$, for the pressure range from 60 to 100 hPa in the triple hydride $LaBH_8$.

We also draw attention to the possible "persistence" of some long-lived metastable phases of metallic hydrogen (such as filamentary and planar phases) into the low-pressure region.

Along with describing homogeneous superconductivity in metallic hydrogen, we analyze in the review inhomogeneous droplet states that arise near the phase boundary of the first-order percolation phase transition between liquid (non-crystalline) metallic and dielectric phases.

From our perspective, despite the conventional nature of superconductivity in the electronic subsystem of metallic hydrogen (via the Eliashberg mechanism), this system possesses a number of unusual (unique) quantum properties.

Diagram of the local crystal structure in the BiO_2 plane of the initial compound $BaBiO_3$, which is a CDW insulator with a checkerboard structure of BiL_2O_6 and BiO_6 octahedra distribution (left figure), and local crystal structure $Ba_{0.5}K_{0.5}BiO_3$ with diagonal chains of complexes BiO_6, embedded in a large percolation cluster of octahedra BiL_2O_6 (right figure) [2]

We draw attention to the analogies between low-dimensional phases of metallic hydrogen and quantum crystals, both in terms of the Lindemann melting parameter and the de Boer quantum parameter, as well as in terms of possible "supersolidity" of metallic hydrogen with coexistence of Bose condensates of Cooper pairs in the electronic subsystem and bi-proton pairs (as in neutron stars) in the ionic subsystem.

2. ORDER PARAMETER DROPLETS IN A LOW-DENSITY ELECTRONIC SYSTEM WITH ATTRACTION IN THE PRESENCE OF STRONG RANDOM POTENTIAL

In papers [4–6], we calculated the properties of a two-dimensional electronic system with low electron density ($n \ll 1$) and strong local Hubbard attraction at the site $|U|/W \geq 1$ (W — band width) in the presence of strong random potential (diagonal disorder) V, uniformly distributed in the range from $-V$ to $+V$. Electronic hops were considered only to neighboring sites of the square lattice with bandwidth $W = 8t$. Calculations were performed on a lattice 24×24 with periodic boundary conditions.

Within the Bogoliubov–de Gennes approach, the emergence of inhomogeneous states of spatially separated Fermi–Bose mixture of Cooper pairs and unpaired electrons was observed, forming bosonic superconducting droplets of different sizes in a matrix of unpaired normal electronic states (see Fig. 2).

An important result of the work is the formation of a large percolation cluster with branched droplet structure, indicating the insulator-superconductor transition [4–6] at electronic densities $n_c \approx 0.31$.

This result is interesting both for understanding the nature of phase transitions and phase diagram of thin films of "dirty" metal [7–9], particularly superconducting stripes of nanostructured aluminum [10], and for experimental implementation of superconducting flux qubits.

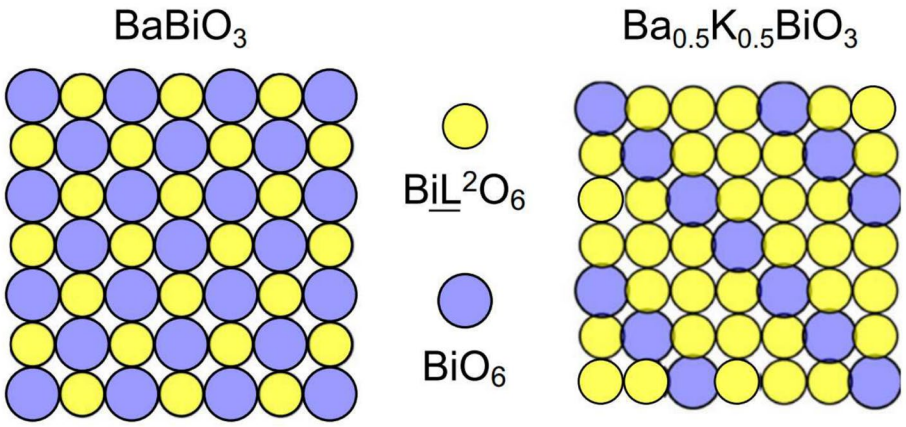

Fig. 1. Diagram of the local crystal structure in the BiO_2 plane of the initial compound $BaBiO_3$, which is a CDW insulator with a checkerboard structure BiL_2O_6 and BiO_6 of octahedra distribution (left figure), and local crystal structure $Ba_{0.5}K_{0.5}BiO_3$ with diagonal chains of complexes BiO_6, embedded in a large percolation cluster of octahedra BiL_2O_6 (right figure) [2]

3. DISCOVERY OF HIGH-TEMPERATURE SUPERCONDUCTIVITY IN METAL HYDRIDES

A breakthrough in increasing the temperature of superconducting transition on the path from high-temperature superconductivity to room-temperature superconductivity dates back to 2014, when researchers from Germany, Russia, and China discovered superconductivity in hydrogen sulfide (H_2S) [11, 12, 13, 14, 15]. At high pressures H_2S first metallizes, and then at pressure $P = 1$ Mbar transition to a superconducting state with $T_c \approx 192$ K takes place.

Moreover, while high-temperature cuprate superconductors cuprate are apparently described by unconventional superconductivity mechanisms based on electron-electron interaction, the superconductivity in hydrogen sulfide has a traditional character and is described by Eliashberg theory [16, 17] for strong electron-phonon interaction.

It should be noted that such high pressures in the range from one to several megabars can be created in special very heavy (multi-ton) diamond anvils. Such diamond anvils are available in institutes in France, USA, and some other countries. In our country, such pressures can be created at the Institute of High Pressure Physics of RAS in Troitsk [11].

This discovery was followed by the discovery of superconductivity at high pressures in H_2S at temperature T_c=203 K, coinciding with the temperature on the surface of Antarctica, and superconductivity in lanthanum hydrides LaH_{10} with $T_c = 250 - 260$ K.

Finally, in 2020, superconductivity with a record temperature to date $T_c = 288$ K (+15°C) was discovered in triple hydride H–C–S with hydrogen dominance at pressure $P = 2.6$ Mbar [18] However, this result has not found independent confirmation.

Around the same time, at the synchrotron source in France, the first convincing experiments were conducted, reliably indicating the transition of pure atomic hydrogen to a metallic state [19–21] at high pressures of about 425 hPa [22].

4. FORMATION OF METALLIC DROPLETS NEAR THE FIRST-ORDER PHASE TRANSITION BOUNDARY BETWEEN METALLIC AND MOLECULAR HYDROGEN IN LIQUID (NON-CRYSTALLINE) STATE

Let us now consider the possibility of droplet formation in metallic hydrogen. Fig. 3 shows the $T-P$-phase diagram of molecular dielectric and atomic (metallic) hydrogen at high pressures. Phase diagram contains 4 phases of molecular and metallic hydrogen interesting for our analysis, namely 2 phases of solid (crystalline) molecular and metallic hydrogen at high pressures and low temperatures, and two phases of liquid molecular and metallic hydrogen at high pressures and high temperatures [11, 23].

Interestingly, with increasing temperature, the phase transition from crystalline to liquid phase for both atomic metallic hydrogen and molecular

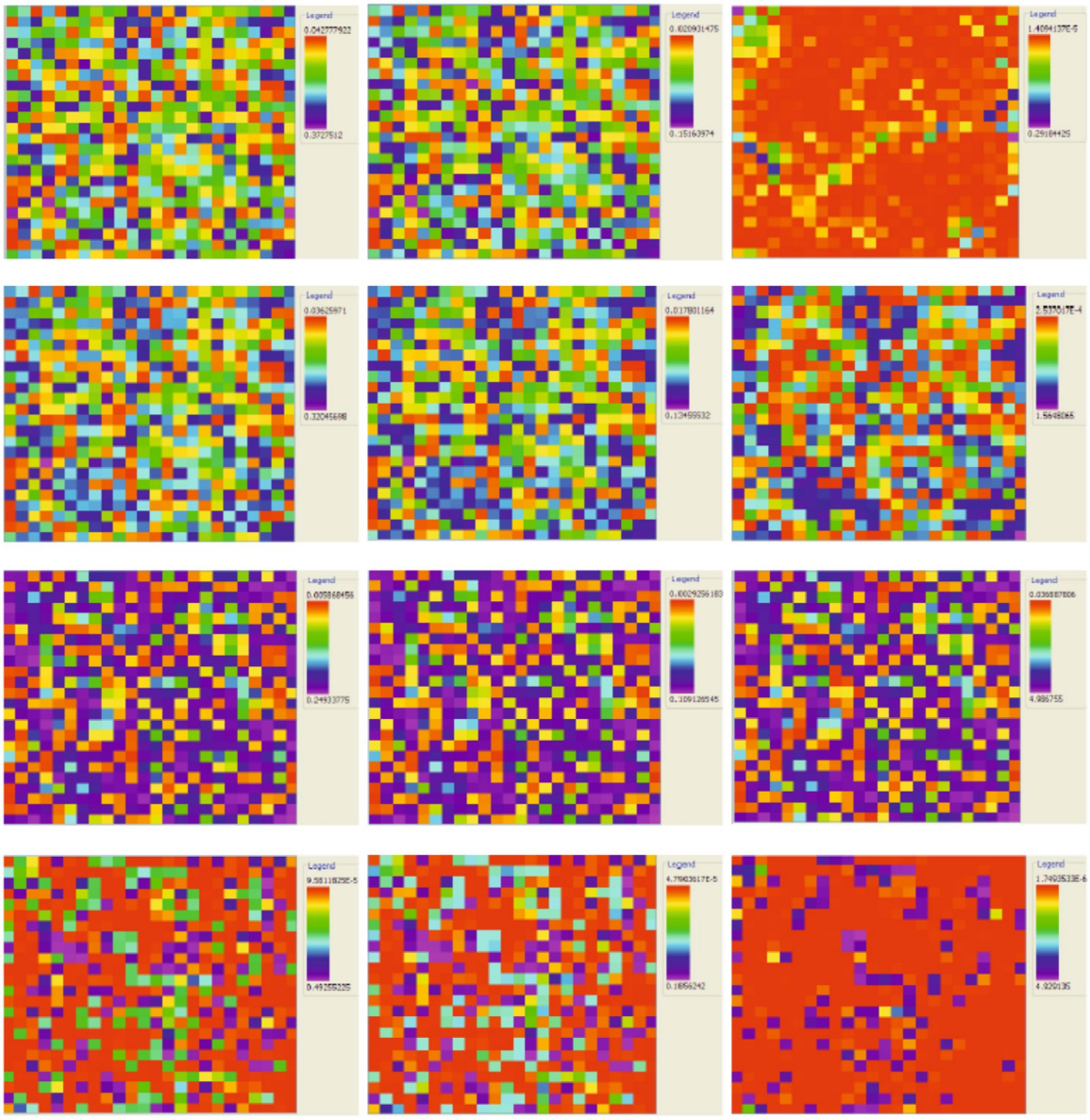

Fig. 2. Two-dimensional distribution of electron density (left column), electron-hole mixing (middle column), and order parameter (right column) at $n = 0.15$ on 24×24 lattice with disorder amplitude $V / t = 10.0$ [4–6]

(dielectric) hydrogen is a first-order phase transition with the formation and growth of nuclei of one phase within another. Note that the formation of liquid droplets and small "ice crystals" around positive and negative ions is well known in the physics of liquid and solid helium.

Also, at high temperatures, the transition from dielectric liquid phase to metallic liquid phase is a first-order phase transition [11]. This transition apparently has a percolation nature with the formation of a complex structure (large cluster) of metallic droplets within the dielectric matrix. Experimental confirmation of the percolation nature of the phase transition and the emergence of conductive metallic droplets comes from the shock wave experiments in deuterium systems [21, 24–27].

5. BASIC MECHANISM OF SUPERCONDUCTIVITY IN METALLIC HYDROGEN AND METAL HYDRIDES

The phonon mechanism of superconductivity, enhanced due to the lightness of the nucleus (small proton mass) in the hydrogen atom, apparently

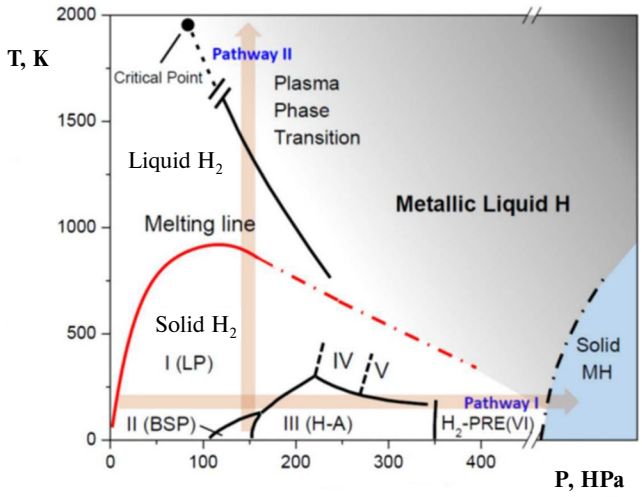

Fig. 3. $T-P$-phase diagram of molecular and atomic metallic hydrogen at high pressures. The phase diagram contains 4 phases of molecular and metallic hydrogen, namely: 2 phases of solid (crystalline) molecular and metallic hydrogen and 2 phases of liquid molecular and metallic hydrogen at high pressures [6, 11, 23]

occurs in metallic hydrogen and in most binary and ternary metal hydrides, such as H_2S, H_3S, LaH_{10}, H–C–S and others.

At the same time, in high-temperature superconductors based on copper-oxygen and in several superconducting systems with low electron density, the dominant superconductivity mechanisms are unconventional non-phonon mechanisms based not on electron-ion, but on electron-electron interaction.

Non-phonon mechanisms include, in particular, the mechanism based on AFM-interaction between copper electron spins in the famous $t-J$ model [28, 29] and Frohlich's plasmon mechanism [30–32], based on the exchange of acoustic plasmons predicted by Nozieres and Pines [33].

Another basic mechanism of unconventional superconductivity is the Kohn–Luttinger mechanism [34–36], based on the presence of the Kohn singularity [37] (Friedel oscillations [38]) in the effective interaction between two electrons through the polarization of the fermionic background.

For metallic hydrogen, the basic mechanism of superconductivity is described by the theory of strong electron-phonon interaction within the framework of Eliashberg theory [39–44]. Calculations using Eliashberg theory by Mazur, Ikhsanov, and M. Kagan [5, 6], as well as other groups [45–48], predict superconductivity for the hexagonal phase of metallic hydrogen at pressure $P = 5$ Mbar with a critical temperature in the range 215–217 K. These calculations are in accordance with earlier ideas expressed by Ashcroft in the United States back in 1968 [49] stating that metallic hydrogen, due to its light nuclear mass (proton) and high Debye frequency, is a very promising candidate for achieving room-temperature superconductivity.

It should be noted that the main challenge for physicists, chemists, and materials scientists today is not so much the task of increasing the critical temperature, but rather the task of lowering the pressure and finding long-lived (even metastable) phases of metallic hydrogen and metal hydrides that are superconducting at normal atmospheric pressure.

Very promising in this regard are the predictions made by Yu. Kagan, Brovman, and Kholas [50, 51] back in the 1970s, suggesting that some low-dimensional phases of metallic hydrogen, particularly the quasi-one-dimensional filamentary phase (proton chains immersed in an electron Fermi liquid) could be stabilized not only at high pressures of several megabars but also realized experimentally as a long-lived metastable phase at lower pressures and even at atmospheric pressure.

Theoretical estimates by Burmistrov and Dubovsky [52], developing the ideas of Yu. Kagan, Brovman, and Kholas, show, in particular, that for the filamentary phase, the region of long-lived metastable states (as a local minimum of a thermodynamic potential) extends at least down to pressures of $P \approx 0.1$ Mbar.

It should be noted that low-dimensional phases of metallic hydrogen, primarily filamentary and planar, share many common features with quantum crystals. In particular, they can have values of the de Boer quantum parameter and Lindemann's quantum melting parameter typical for the physics of supersolidity of helium quantum crystals and the ideas from the classical work of Andreev–Lifshitz [53].

Developing Ashcroft's ideas [54], one of the authors of the present paper (M. Yu. K.) [55, 56] proposed the idea of a possible non-trivial superfluid state in metallic hydrogen at high pressures, resembling the superfluidity of neutron stars.

In this state, the coexistence of two Bose-condensates is possible — a condensate of Cooper pairs in the electronic subsystem and a condensate of

biprotonic pairs on one (or adjacent) chains (planes) in the ionic subsystem.

It should also be noted that additional possibilities for pressure reduction in metalic hydrides on the path to technical applications of room-temperature superconductivity are related with chemical composition.

It turns out that increasing the complexity of metal hydride composition, and particularly the transition from binary to ternary hydrides [28], contributes to effective pressure reduction while maintaining high critical temperatures.

Recently (summer 2023), South Korean technologists announced the synthesis of a metal hydride with room-temperature critical temperature at atmospheric pressure. Unfortunately, however, their results have not been confirmed by other groups.

6. NEW RESULTS ON METALLIC HYDROGEN AND METAL HYDRIDES

In this section, we briefly announce our latest results related to the possibility of pressure reduction in complex metal hydrides using $LaBH_8$ as an example [28]. In particular, we demonstrate the curve of critical temperature dependence on pressure with negative derivative (i.e. $dT_c / dP < 0$) for the pressure range from 60 to 100 hPa in the ternary hydride $LaBH_8$.

For calculations of T_c we used the the system of the Eliashberg equations [39, 40, 41, 42, 43, 44] with a correction to the electron chemical potential [57, 58], which allows describing the enhancement effect for T_c when the density of states peak approaches the Fermi energy [58, 59, 60].

The independent variable in this system is the frequency ω, measured in energy units (eV). The dependent variables form a set $\{\varphi(\omega), Z(\omega), \chi(\omega)\}$, where φ is the order parameter, Z is the electron mass renormalization function, χ is the chemical potential shift. $[\varphi] = [\chi] =$ eV, Z is a dimensionless quantity. The numerical parameters of the system form a set $\{T, \mu^*, \mu, \omega_c\}$, where T is temperature, $[T] = K$; μ^* is screened Coulomb potential, $[\mu^*] = 1$; μ is the chemical potential of electrons (we assume it equal to the Fermi energy E_F), $[\mu] =$ eV; ω_c is the effective energy range of Coulomb interaction (usually we take $\sim 3\omega_D$, where ω_D — Debye frequency). Functional parameters: $\{\alpha^2 F(\omega), N_0(E)\}$, where $\alpha^2 F(\omega)$ is the Eliashberg function; $N_0(E) = N(E) / N(0)$ is the normalised electron density of states, where $N(E)$ is the density of states, $N(0)$ is the density of states at the Fermi level. Functions $\alpha^2 F(\omega)$ and $N_0(E)$ are given in tabulated form and were calculated in advance using density functional theory implemented in the Quantum Espresso package [61]. This work used Optimized Normconserving Vanderbilt Pseudopotentials (ONCVPSP) version 0.4.1 [62] and the PBE exchange-correlation functional. The EPW program was used to calculate the Eliashberg spectral function for interpolation of the electron-phonon matrix using Wannier functions [63].

To solve this system on the frequency axis, a grid of positive Matsubara frequencies is chosen

$$\{\omega_n = \pi k T(2n+1)\}_{n=0}^{M},$$

where $n \in [0, M]$, and variables $\{\varphi(\omega), Z(\omega), \chi(\omega)\}$ are calculated on this grid: $\{\varphi_n, Z_n, \chi_n\}_{n=0}^{M}$. The system of equations in this case has the form

$$\varphi_n = \frac{\pi}{\beta}\sum_{n=0}^{M}\{\lambda_{nm}^{(+)} - 2\mu^*\theta\left(\omega_c - \left|\omega_m\right|\right)\}\varphi_m \cdot N_m$$

$$Z_n = 1 + \frac{\pi}{\beta}\frac{1}{\omega_n}\sum_{m=0}^{M}\lambda_{nm}^{(-)}\omega_m Z_m \cdot N_m \qquad (1)$$

$$\chi_n = -\frac{\pi}{\beta}\sum_{m=0}^{M}\{\lambda_{nm}^{(+)} - 2\mu^*\theta\left(\omega_c - \left|\omega_m\right|\right)\} \cdot P_m$$

where

$$\beta = 1 / kT,$$

$$\lambda_{nm}^{(\pm)} = \lambda(n-m) \pm \lambda(n+m+1),$$

$$\lambda(n) = 2\int_0^{\omega_D}\frac{\omega \cdot \alpha^2 F(\omega)}{\omega^2 + (2\pi n k_B T)^2}d\omega,$$

$$N_m = N_m(\varphi_m, Z_m, \chi_m),$$

$$P_m = P_m(\varphi_m, Z_m, \chi_m),$$

$$N_m(\varphi, Z, \chi) =$$

$$= \pi^{-1}\int_{-\mu}^{+\infty} N_0(E)\frac{1}{(E+\chi)^2 + Z^2\omega_m^2 + \varphi^2}dE,$$

$$P_m(\varphi, Z, \chi) =$$

$$= \pi^{-1} \int_{-\mu}^{+\infty} N_0(E) \frac{E + \chi}{(E + \chi)^2 + Z^2 \omega_m^2 + \varphi^2} dE,$$

$[N_m] = \text{eV}^{-1}$, P_m is a dimensionless quantity.

The desired quantity, which determines the superconducting transition temperature T_c, is $\Delta_0 = \varphi(\omega_0) / Z(\omega_0)$, with the dimension of eV (T_c is determined from the condition $\Delta_0(T) = 0$ at $T \geq T_c$).

The calculation results for T_c of the triple hydride $LaBH_8$, performed for various pressures, are shown in Fig. 4, and the reduced density of states $N_0(E)$ — in Fig. 5. The calculations were carried out in the pressure range from 60 to 100 hPa. For lower pressures, this compound may be unstable. The calculations were performed using two methods: by solving the "classical" Eliashberg equation system, which does not take into account the correction to the chemical potential of electrons, and the electronic density of states is not present in the equations (see, for example, [64]), and by solving system (1). The calculations were performed for $\mu = 0.09, \omega_D = 0.25\,\text{eV}$ and $M = 18$ (i.e., 19 positive Matsubara frequencies were taken).

The decrease in T_c with increasing pressure, starting from 80 hPa, was shown by both methods. The decrease in T_c, and even in a larger pressure range, is also shown by the results of [28] (and the result of [65] agrees well with our calculations). Taking into account the correction to the chemical potential of electrons gives an increase in T_c for all pressures. This increase is caused by the presence of a broad peak in the density of electronic states, localized at a distance of the order of Debye energy from the Fermi level (see Fig. 5). The behavior of $N_0(E)$ at energies greater than ω_D, practically does not affect the value of T_c. With decreasing pressure, there is an increase in this peak and, accordingly, an increase in the calculated value of T_c.

7. CONCLUSION

Hopes for the implementation of room-temperature superconductivity and its technical applications require the search for stable or metastable phases of metallic hydrogen and metal hydrides that are superconducting at lower pressures. The pressure reduction may be associated with both the increasing complexity of metal hydrides' chemical composition and the "dragging in" of low-dimensional phases of pure metallic hydrogen (primarily filamentary and planar) in the region of metastable long-lived states at atmospheric pressure as a local minimum of the thermodynamic potential due to the time-consuming processes of quantum nucleation when tunneling through a high barrier in configuration space. As a first result towards implementing the task of pressure reduction in metal hydrides, we demonstrate the negative sign of the derivative $dT_c / dP < 0$ for the pressure range from 60 to 100 hPa in the ternary hydride $LaBH_8$.

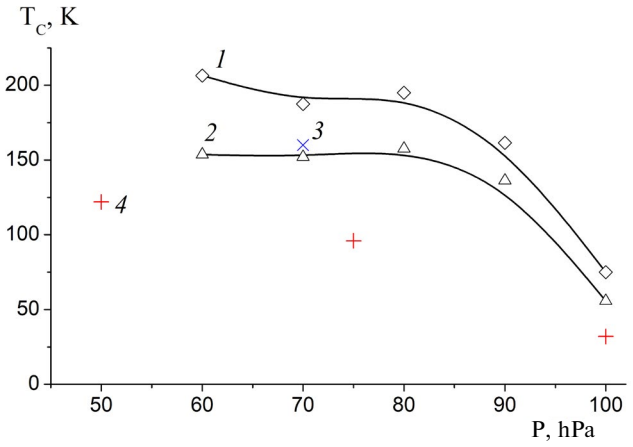

Fig. 4. Calculated dependence of T_c on pressure for $LaBH_8$, calculated in various ways: 1 – solution of system of equations (1); of 2 – solution of Eliashberg equations without correction to electron chemical potential; 3 – results from [65]; 4 – results from [28]

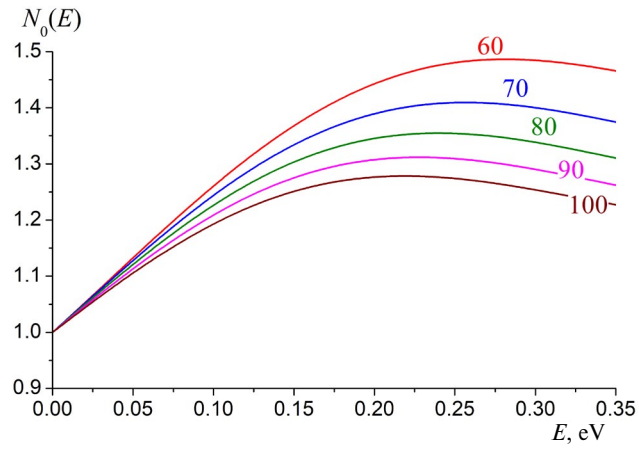

Fig. 5. Normalised density of states $N_0(E)$ for $LaBH_8$, calculated for different pressures: pressure values in hPa are indicated next to the curves. Zero energy corresponds to the Fermi level

The physics of inhomogeneous droplet structures in percolation phase transitions between dielectric and conducting phases of liquid molecular and liquid metallic hydrogen, as well as the dielectric-superconductor transition in low-density electronic systems with attraction and "dirty" metallic films [7–9], is of great interest not only for astrophysical observations [20, 25, 66] and shock wave experiments in extreme states of matter, but also for superconducting nanoelectronics [10] and possible superconducting implementation of quantum computing.

FUNDING

M. Kagan and R. Ikhsanov thank the HSE University Centre for Basic Science Research for its support. The study was conducted using the HSE University supercomputer complex [67], resources of the high-performance computing center of MEPhI.

REFERENCES

1. A. Menushenkov, K. V. Klementev, A. V. Kuznetsov, and M. Yu. Kagan, ZHETP 120, 700 (2001).

2. A. Menushenkov, A. V. Kuznetsov, K. V. Klementiev, and M. Yu. Kagan, J. Supercond. Nov. Magn. 29, 701 (2016).

3. M. Yu. Kagan, K. I. Kugel, and A. L. Rakhmanov, Phys. Reports 916, 1 (2021)

4. M. Yu. Kagan, E. A. Mazur, JETP 159, 696 (2021).

5. E. A. Mazur, R. Sh. Ikhsanov, and M. Yu. Kagan, J. Phys.: Conf. Series, 2036, 012019 (2021).

6. M. Yu. Kagan, S. V. Aksenov, A. V. Turlapov, R. Sh. Ikhsanov, K. I. Kugel, E. A. Mazur et al., JETP Letters 117, 754 (2023).

7. A. M. Goldman and N. Markovic, Phys. Today 51, 39 (1998).

8. D. B. Haviland, Y. Liu, and A. M. Goldman, Phys. Rev. Lett. 62, 2180 (1989).

9. E. Z. Kuchinsky, I. A. Nekrasov, M. V. Sadovsky, Physics-Uspekhi 53, 325 (2012).

10. N. Grunhaupt et al., Nature Mater. 18, 1816 (2019).

11. A. N. Utyuzh, A. Mikheenkov, Physics-Uspekhi 187, 953 (2017).

12. I. A. Troyan, D. V. Semenok, A. G. Ivanova, A. G. Kvashnin, D. Zhou, A. V. Sadakov, O. A. Sobolevsky, V. M. Pudalov, I. Lyubutin, A. R. Oganov, Physics-Uspekhi 192, 799 (2022).

13. M. I. Eremets, A. P. Drozdov, Physics-Uspekhi 186, 1257 (2016).

14. D. Duan et al., Sci. Rep. 4, 6968 (2014).

15. A. Drozdov et al., Nature 525, 73 (2015).

16. G. M. Eliashberg, JETP 38, 966 (1960).

17. M. V. Sadovsky, arxiv cond-mat. 2106.09948, 18 Jun (2021).

18. E. Snider et al., Nature 586, 373 (2020).

19. E. Wigner and H. B. Huntington, J. Chem. Phys. 3, 764 (1935)

20. A. A. Abrikosov, Astron. J. 31, 112 (1954).

21. R. Dias, I. F. Silvera, Science 355, 715 (2017).

22. P. Loubyere et al., Nature 577, 631 (2020).

23. M. Houtput, J. Tempere, and I. F. Silvera, Phys. Rev. B 100, 134106 (2019).

24. M. D. Knudson et al., Science 348, 1455 (2015).

25. V. E. Fortov et al., Phys. Rev. Lett. 99, 185001 (2007).

26. G. W. Collins et al., Science 281, 1178 (1998).

27. M. Celliers et al., Phys. Rev. Lett. 84, 5564 (2000).

28. S. D. Cataldo, Ch. Heil, W. von der Linden, and L. Boeri, Phys. Rev. B 104, L020511 (2021).

29. M. Yu. Kagan and T. M. Rice, J. Phys.: Condens. Matter 6, 3771 (1994).

30. H. Frohlich, J. Phys. C 1, 544, Letters to Editor (1968).

31. J. Ruhman and P. A. Lee, Phys. Rev. B 96, 235107 (2017).

32. J. Ruhman and P. A. Lee, arxiv cond-mat 1605.01737, 7 June (2016).

33. D. Pines, P. Nozieres, The Theory of Quantum Liquids, Benjamin, New York (1966).

34. M. Yu. Kagan, M. M. Korovushkin, V. A. Mitskan, Physics-Uspekhi 185, 785 (2015).

35. M.Yu. Kagan, A.V. Chubukov, JETP Letters 47, 525 (1988).

36. W. Kohn and J. M. Luttinger, Phys. Rev. Lett. 15, 524 (1965).

37. W. Kohn, Phys. Rev. Lett. 2, 393 (1959).

38. H. Friedel, Adv. Phys. 3, 446 (1954).

39. O. V. Dolgov, R. K. Kremer, J. Kortus et al., Phys. Rev. B 72, 024504 (2005).

40. Z. Zhang, T. Cui, M.J. Hutcheon et al., Phys. Rev. Lett. 128, 047001 (2022).

41. P. B. Allen and R. C. A. Dynes, Tech. Rev. 7, TCM4 (1974).

42. P. B. Allen and R. C. A. Dynes Phys. Rev. B 12, 905 (1975).

43. F. Marsiglio and J. Carbotte, Physica C: Superconductivity 1, 73 (2008).

44. J. Carbotte, Rev. Mod. Phys. 62, 1027 (1990).

45. R. Szczesniak, Acta Physica Polonica A 109, 179 (2006).

46. A. Durajski, Sci. Reports 6, 38570 (2016).

47. N. A. Kudryashov, A. A. Kutukov, E. A. Mazur, JETP Letters 104, 488 (2016).

48. I. A. Kruglov, D. Semenok, H. Song et al., Phys. Rev. B 101, 024508 (2020).

49. N. W. Ashcroft, Phys.Rev. Lett. 21, 1748 (1968).

50. E. G. Brovman, Yu. M. Kagan, A. Holas, JETP 61, 2429 (1972).

51. E. G. Brovman, Yu. M. Kagan, A. Holas, V. V. Pushkarev, JETP Letters 18, 269 (1973).

52. S. N. Burmistrov and L. B. Dubovskii, arxiv condmat 1611.02593, 8 November (2016).

53. A. F. Andreev and I. M. Lifshitz, JETP 29, 1107 (1969).

54. N. W. Ashcroft, J. Phys. A 36, 6137 (2003).

55. M. Yu. Kagan, JETP Letters 103, 822 (2016).

56. M. Yu. Kagan and A. Bianconi, Condens. Matter 4, 51 (2019).

57. W. E. Pickett, Phys. Rev. B 26, 1186 (1982).

58. V. N. Grebenev, E. A. Mazur, Low Temperature Physics 13, 479 (1987).

59. A. S. Aleksandrov, V. F. Elesin, M. P. Kazeko, Soviet Physics Solid State 21, 2062 (1979).

60. N. A. Kudryashov, A. A. Kutukov, E. A. Mazur, JETP Letters 104, 488 (2016).

61. P. Giannozzi, S. Baroni, N. Bonini et al., J.Phys.: Condens. Matter 21, 395502 (2009).

62. D. R. Hamann, Phys. Rev. B 88, 085117 (2013).

63. S. Ponce, E.R. Margine, C. Verdi, and F. Giustino, Comput. Phys. Comm. 209, 116 (2016).

64. R. Sh. Ikhsanov, E. A. Mazur, M. Yu. Kagan, Proceedings of the Ufa Scientific Center of RAS No. 1, 49 (2023).

65. Z. Zhang, T. Cui, and M. J. Hutcheon et al., Phys. Rev. Lett. 128, 047001 (2022).

66. V.S. Filinov, V.E. Fortov, M. Bonits, P.R. Levashov, JETP Letters 74, 422 (2001).

67. S. Kostenetskiy, R. A. Chulkevich, V. I. Kozyrev, J. Phys.: Conf. Ser. 1740, 012050 (2021).